Available online at www.sciencedirect.com
ScienceDirect
Journal of Molecular Catalysis A: Chemical 282 (2008) 107–116
JOURNAL OF MOLECULAR CATALYSIS A: CHEMICAL
www.elsevier.com/locate/molcata

Comparison of olefin polymerization behavior of sterically crowded tris(pyrazolyl)borate group 4 metal complexes

Kenji Michiue [a], Richard F. Jordan [b,*]

[a] *R&D Center, Mitsui Chemicals, Inc., 580-32 Nagaura, Sodegaura-City, Chiba 299-0265, Japan*
[b] *Department of Chemistry, The University of Chicago, 5735 South Ellis Avenue, Chicago, IL 60637, USA*

Received 14 August 2007; accepted 15 November 2007
Available online 11 January 2008

Abstract

The ethylene polymerization and ethylene/α-olefin copolymerization behavior of the sterically crowded tris(pyrazolyl)borate group 4 metal complexes $Tp^{Ms*}TiCl_3$ (**1**, Tp^{Ms*} = HB(3-mesitylpyrazolyl)$_2$(5-mesitylpyrazolyl)$^-$), $\{K[Tp^{Ms*}TiCl_3]\}_2$ (**2**), $Tp^{Ms*}TiCl_2$(O-2,4,6-^{t}Bu$_3$-Ph) (**3**), $Tp^{Ms*}ZrCl_3$ (**4**), $Tp^{Ms}ZrCl_3$ (**5**, Tp^{Ms} = HB(3-mesitylpyrazolyl)$_3^-$), and $Tp^{Ms*}HfCl_3$ (**6**) were studied with dried-MAO activation in toluene solution. These catalysts all produce very high molecular weight ($M_v > 10^6$) linear polyethylene. Zirconium catalyst **5** excels in productivity in ethylene homopolymerization and ethylene/1-hexene copolymerization, molecular weight, and hexene incorporation ability. Catalyst **5** produces moderately alternating ethylene/1-hexene copolymer (41 mol% hexene) with ultra-high molecular weight ($M_w = 1.3 \times 10^6$), narrow molecular weight distribution ($M_w/M_n = 2.2$) and narrow composition distribution with high efficiency.

Keywords: Olefin polymerization catalyst; Post-metallocene catalyst; Tris(pyrazolyl)borate; Titanium; Zirconium; Hafnium; Aryloxide

1. Introduction

Following the discovery of metallocene catalysts, research on single-site olefin polymerization catalysts based on well-defined organometallic complexes has been actively pursued and many high-performance metallocene [1] and post-metallocene [2] catalysts have been discovered. A significant advantage of single-site catalysts compared to Ziegler-Natta catalysts is that they enable precise control of polymer microstructure through manipulation of the active site structure via ligand design. This feature opens up the possibility of developing high-performance catalysts that can create high-value polyolefins that are not accessible by conventional catalysts.

Tris(pyrazolyl)borate ligands are attractive candidates for ancillary ligands for single-site catalysts, because they are mono-anionic, 6-electron donors like cyclopentadienyl (Cp) ligands [3], and their properties can be tuned by varying the substituents on the pyrazolyl rings. Early studies showed that MAO-activated group 4 metal Tp'MCl_3 complexes (Tp' = generic tris(pyrazolyl)borate) that contain the simple Tp' ligands HB(pyrazolyl)$_3^-$ (Tp) or HB(3,5-Me$_2$-pyrazolyl)$_3^-$ (Tp*) exhibit poor productivity for ethylene, ethylene/α-olefin, and styrene polymerization, and produce polymers with broad molecular weight distributions (MWDs) [4,5]. However, the productivity of Tp'MX_3/MAO catalysts is strongly influenced by the steric properties of the Tp' ligand. In particular, Tp'MCl_3 complexes that contain mesityl-substituted Tp' ligands, such as HB(3-mesityl-pyrazolyl)$_2$(5-mesityl-pyrazolyl)$^-$ (Tp^{Ms*}) and HB(3-mesityl-pyrazolyl)$_3^-$ (Tp^{Ms}) exhibit very high productivities in ethylene polymerization, which are comparable to those of zirconocene catalysts [6–9]. Moderately crowded Tp'MCl_3 complexes that contain *tert*-butyl-, neopentyl-, or phenyl-substituted Tp' ligands exhibit moderate productivity [10].

Group 4 metal Tp'MCl_2(OR)/MAO catalysts have also been studied. Early work showed that these catalysts give low productivity [4a,11], but recently it was discovered that Tp'Ti(OR)$TiCl_2$/MAO catalysts that contain Tp and Tp* ligands exhibit high productivity when the alkylaluminum concentration is low [12].

Chain growth in Tp'MCl_3/MAO-catalyzed olefin polymerization is assumed to proceed by a normal insertion

* Corresponding author. Tel.: +1 773 702 6429; fax: +1 773 702 0805.
E-mail address: rfjordan@uchicago.edu (R.F. Jordan).

1381-1169/$ – see front matter © 2007 Elsevier B.V. All rights reserved.
doi:10.1016/j.molcata.2007.11.023

mechanism. However, the active species in these systems have not been identified. One possibility is that the active species are Tp'M(X)(R)$^+$ cations (X = Cl, R or other anionic ligand), analogous to the Cp_2MR^+ active species in metallocene catalysts. The Tp*Zr$(CH_2Ph)_2^+$ cation has been characterized and, interestingly, rearranges to the bis-pyrazolyl species $\{PhCH_2HB(\mu\text{-pz*})_2\}Zr(CH_2Ph)(pz*)^+$ (pz* = 3,5-Me_2-pyrazole) at low temperature [13]. Both of these species function as single component ethylene polymerization catalysts. These results, and the general ability of Tp' complexes to rearrange by borotropic shifts [6a,9], suggest that active species formation in Tp'M catalysts may be more complicated than in metallocene systems.

The dominant chain transfer mechanism for Tp'MCl_3/MAO catalysts is chain transfer to MAO and $AlMe_3$ [6a,9]. Therefore, molecular weight can be controlled from low to ultra-high molecular weight by varying the alkyl aluminum concentration, and Al-terminated polymers, which are useful for the production of functional polymers and block copolymers [14], can be easily obtained [8]. Chain transfer to Al can result in broad MWDs when low cocatalyst levels are used [6a,9]. Beta-hydrogen transfer is usually insignificant in these catalysts.

Interesting results have been observed in Tp'MCl_3/MAO-catalyzed ethylene/α-olefin copolymerization. Tp^{Ms*}Ti(IV)Cl_3/MAO exhibits low hexene incorporation in ethylene/1-hexene copolymerization [15], but the analogous Ti(III) catalyst $\{K[Tp^{Ms*}Ti(III)Cl_3]\}_2$ [8], and zirconium catalysts such as Tp*$ZrCl_3$/MMAO [4a], and $Tp^{Ms}ZrCl_3$/MAO [9] exhibit high comonomer incorporation. Ultra-high molecular weight ethylene/1-hexene copolymer, which is difficult to produce by conventional catalysts with high efficiency under commercially practical conditions, was obtained with $Tp^{Ms}ZrCl_3$/MAO (e.g. 240 kg/(mmol Zr·h), $M_w = 1.6 \times 10^6$, 18 mol% hexene) [9].

An attractive feature of Tp'MCl_3 catalysts is their robustness at high polymerization temperatures (T_ps). Productivities of Tp'MX_3 catalysts remain high at T_ps greater than 70 °C [4d,6a,8,9], and high molecular weight polyethylene (PE) and ethylene/α-olefin copolymers can be prepared at these temperatures. The versatile features of group 4 metal Tp'MX_3 catalysts make them attractive potential candidates for commercial application [16].

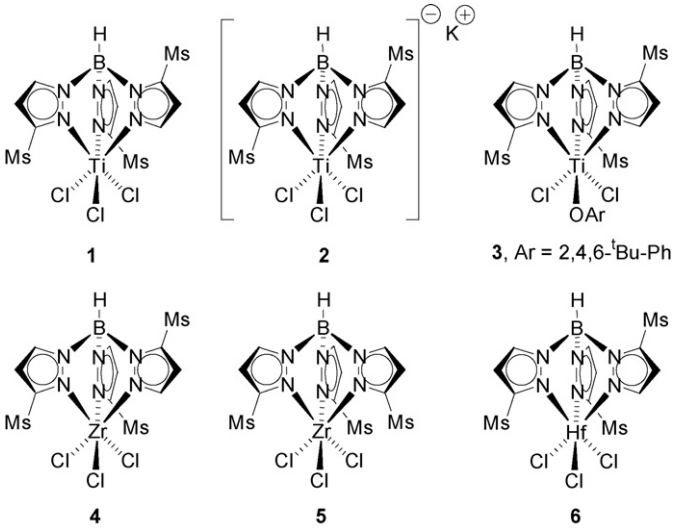

Fig. 1. Tp'MX_3 catalysts employed in this study. Ms = mesityl = 2,4,6-Me_3-Ph.

While these results are intriguing, structure/performance relationships for Tp'MX_3 catalysts are not well understood. Therefore, in the present study, we have evaluated a set of Tp'MX_3 catalysts under identical conditions using a parallel pressure reactor. We have studied six catalysts, Tp^{Ms*}Ti(IV)Cl_3 (**1**), $\{K[Tp^{Ms*}Ti(III)Cl_3]\}_2$ (**2**), $Tp^{Ms*}TiCl_2$(O-2,4,6-^{t}Bu_3-Ph) (**3**), $Tp^{Ms*}ZrCl_3$ (**4**), $Tp^{Ms}ZrCl_3$ (**5**), $Tp^{Ms*}HfCl_3$ (**6**), which are shown in Fig. 1, under commercially relevant solution polymerization conditions using dried MAO (DMAO) as the activator. The results provide a phenomenological picture of how the metal (Ti, Zr, Hf), Ti oxidation state, Tp' ligand structure, and the presence of an aryloxide substituent influence the olefin polymerization performance for this class of catalysts.

2. Experimental

2.1. General

All manipulations were performed using dry box or Schlenk techniques under a purified N_2 atmosphere, or on a high-vacuum line, unless otherwise indicated.

2.1.1. Materials

Nitrogen was purified by passage through columns containing activated molecular sieves and Q-5 oxygen scavenger. Et_2O and THF-d_8 were distilled from sodium benzophenone ketyl. Hexane and toluene were purified by passage through columns of activated alumina and BASF R3-11 oxygen scavenger. Solvents were stored under N_2 or vacuum prior to use. 2,4,6-Tri-*tert*-butylphenol and potassium bis(trimethylsilyl)amide were purchased from Aldrich. Dry toluene employed as a polymerization solvent was obtained from Wako Pure Chemical Industries, Ltd., and used without further purification. Toluene used for dissolving precatalysts was distilled from Na/K. 1-Hexene was obtained from Mitsubishi Chem. Co. and distilled from Na/K. Methylalmoxane (MAO) was purchased from Albemarle Corporation as a 1.2 M toluene solution. This solution was dried under vacuum to remove the toluene and a substantial fraction of the $AlMe_3$, to produce "dried MAO" (DMAO). Ethylene was obtained from Sumitomo Seika Co. Cp_2ZrCl_2 was purchased from Wako Pure Chemical Industries, Ltd.

2.1.2. Characterization of ligands and complexes

NMR spectra were recorded on a Bruker DRX400 spectrometer in flame-sealed tubes at 23 °C. ^{1}H and ^{13}C chemical shifts were determined by reference to the residual ^{1}H and ^{13}C solvent signals. Coupling constants are reported in Hz. Elemental analyses were performed by Midwest Microlab. FD-MS spectra were recorded on a JEOL SX-102A instrument.

2.1.3. Polymer characterization

Melt transition temperatures (T_m) of the polyethylenes (PEs) were determined by differential scanning calorimetry (DSC) with a Shimadzu DSC-60 instrument. The polymer samples

were heated at 50 °C/min from 20 to 200 °C, held at 200 °C for 5 min, and cooled to 0 °C at 20 °C/min. The samples were held at this temperature for 5 min, and then reheated to 200 °C at 10 °C/min. The reported T_m was determined from the second heating scan unless otherwise noted. Intrinsic viscosities [η] were measured in decalin at 135 °C using an Ubbelohde viscometer (25 mg PE/25 mL decalin). Viscosity average molecular weights (M_v) were calculated from the equation $[\eta] = (6.2 \times 10^{-4})M_v^{0.7}$ [17].

Molecular weights (M_w and M_n) and molecular weight distributions (MWDs) of ethylene/hexene copolymers in Table 2 were determined using a Waters GPC2000 gel permeation chromatograph equipped with four TSKgel columns (two sets of TSKgelGMH$_6$-HT and two sets of TSKgelGMH$_6$-HTL) at 140 °C using polystyrene calibration. *o*-Dichlorobenzene (ODCB) was used as the solvent.

CFC analyses were performed on a Mitsubishi Yuka CFC T-150A instrument equipped with three columns (Shodex AT-806MS, Showa Denko KK) at 140 °C, using ODCB as the solvent at a flow rate of 1.0 mL/min. Elution of the polymer with ODCB was carried out every 5 °C from 0 to 140 °C. The polymer concentration in each eluent was monitored by an online IR detector (1ACVF, Miran), and M_w, M_n and MWD were determined using polystyrene calibration.

The α-olefin content of the ethylene/α-olefin copolymers was measured by ^{13}C NMR on a JEOL EX400 or GSX270 instrument, using ODCB with 20% benzene-d_6 as a solvent at 110 °C.

2.2. Complex synthesis

Complexes **1** [6a], **2** [8], **4** [7,9], **5** [9], and **6** [9] were prepared by literature procedures.

2.2.1. Preparation of Tp^{Ms*}Ti(O-2,4,6-^{t}Bu$_3$-Ph)Cl$_2$ (**3**)

2.2.1.1. Preparation of K[O-2,4,6-^{t}Bu$_3$-Ph]. A solution of potassium bis(trimethylsilyl)amide (0.690 g, 3.46 mmol) in Et$_2$O (70 mL) was canula-transferred at 0 °C to 2,4,6-tri-*tert*-butylphenol (1.00 g, 3.81 mmol). The mixture was gradually warmed to 20 °C and stirred at this temperature for 1 h. The resulting thick white slurry was taken to dryness under vacuum yielding an ivory solid. This material was washed with hexane (ca. 300 mL in three portions) and dried under vacuum to give K[O-2,4,6-^{t}Bu$_3$-Ph] (1.02 g, 98%) as a white solid. ^{1}H NMR (THF-d_8): δ 6.82 (s, 2H, Ph), 1.40 (s, 18H, 2,6-^{t}Bu), 1.20 (s, 9H, 4-^{t}Bu).

*2.2.1.2. Preparation of Tp^{Ms*}Ti(O-2,4,6-^{t}Bu$_3$-Ph)Cl$_2$ (**3**).* A Schlenk flask was charged with **1** (1.00 g, 1.39 mmol) and K[O-2,4,6-^{t}Bu$_3$-Ph] (0.419 g, 1.39 mmol), and toluene (150 mL) was added at 20 °C. The mixture was stirred at 20 °C and immediately turned to a deep blue solution. The mixture was stirred at 20 °C for 12 h to produce a suspension of a white solid in a deep brown supernatant. The mixture was stirred for 9 days. The suspension was filtered through celite, affording deep brown filtrate. The filtrate was concentrated to 20 mL and stored at −37 °C to yield a brown powder, which was collected by filtration, washed with hexane, and dried under vacuum to yield pure **3** as brown powder (956 mg, 72.8%). Anal. Calcd for $C_{54}H_{69}N_6BCl_2OTi$: C, 68.43; H, 7.34; N, 8.87. Found: C, 67.92; H, 7.36; N, 7.93. ^{1}H NMR (THF-d_8): δ 7.92 (d, $^3J_{HH}$ = 1.2, 1H, pz-H3), 7.59 (d, $^3J_{HH}$ = 1.4, 1H, pz-H5), 7.46 (d, $^3J_{HH}$ = 1.4, 1H, pz-H5), 7.29 (d, $^3J_{HH}$ = 2.3, 1H, *m*-Ph), 7.15 (d, $^3J_{HH}$ = 2.4, 1H, *m*-Ph), 7.05 (s, 1H, Ms *m*-H), 6.96 (s, 1H, Ms *m*-H), 6.74 (s, 2H, Ms *m*-H), 6.69 (s, 1H, Ms *m*-H), 6.62 (s, 1H, Ms *m*-H), 6.11 (d, $^3J_{HH}$ = 1.8, 1H, pz-H4), 6.09 (d, $^3J_{HH}$ = 1.8, 1H, pz-H4), 5.91 (d, $^3J_{HH}$ = 1.8, 1H, pz-H4), 2.37 (s, 3H, Ms *p*-Me), 2.32 (s, 3H, Ms *p*-Me), 2.25 (s, 3H, Ms *p*-Me), 2.23 (s, 3H, Ms *o*-Me), 2.19 (s, 3H, Ms *o*-Me), 2.14 (s, 3H, Ms *o*-Me), 1.68 (s, 3H, Ms *o*-Me), 1.65 (s, 3H, Ms *o*-Me), 1.53 (s, 3H, Ms *o*-Me), 1.35 (s, 9H, Ph *o*-^{t}Bu), 1.29 (s, 9H, Ph *o*-^{t}Bu), 0.81 (s, 9H, Ph *p*-^{t}Bu). ^{13}C{^{1}H} NMR (THF-d_8): δ 172.3 (O*C*Ph), 158.0 (pz 3-C), 157.3 (pz 3-C), 146.9, 146.6, 145.3, 140.7, 140.0, 139.5, 139.3, 138.6, 138.5, 138.2, 138.0, 137.6, 137.2, 136.4, 136.3, 131.9, 131.3, 129.0, 128.84, 128.75, 128.5, 128.0, 127.9, 124.6, 122.9, 108.7, 107.1, 106.9, 38.6, 37.8, 35.1, 33.9, 33.2, 31.8, 23.5, 21.9, 21.38, 21.35, 21.32, 21.25, 21.19, 19.8. FD-MS: *m*/*z* = 947 (M+).

2.3. Polymerization procedure

Polymerization reactions were performed in a parallel pressure reactor (Argonaut Endeavor® Catalyst Screening System) containing eight reaction vessels (15 mL) each equipped with a mechanical stirrer and monomer feed lines. A toluene solution of DMAO was loaded in each vessel, and a stainless steel manifold equipped was attached. *For ethylene polymerization*, the nitrogen atmosphere was replaced with ethylene and the solution was saturated with ethylene at the polymerization pressure and thermally equilibrated at the polymerization temperature (T_p). *For ethylene/1-hexene copolymerization*, 1-hexene was injected into each vessel after the solution was saturated with ethylene at the T_p. *For ethylene/propylene copolymerization*, the nitrogen atmosphere was replaced with propylene and the reaction vessels were pressurized with propylene (3.87 atm at 25 °C). The solution was heated to the T_p and thermally equilibrated, and ethylene was introduced into the reactor up to the polymerization pressure. *In all cases* the polymerization was started by addition of a toluene solution of the metal complex (0.20 mL toluene solution of complex followed by 0.25 mL toluene wash). The total volume of the reaction mixture was 5 mL for all polymerizations. The pressure was kept constant by feeding ethylene on demand. After the reaction, the polymerization was stopped by addition of excess isobutyl alcohol. The resulting mixture was added to acidified methanol (45 mL containing 0.5 mL of concentrated HCl). The polymer was recovered by filtration, washed with methanol (2 mL × 10 mL) and dried in a vacuum oven at 80 °C for 10 h.

3. Results and discussion

3.1. Synthesis of **3**

The reactions of **1** with several alkali metal alkoxides were studied as possible routes to Tp^{Ms*}TiCl$_2$(OR) complexes. Complex **1** does not react with NaOMe in toluene at 20 °C, in contrast

to Tp*$TiCl_3$, which reacts to yield Tp*$TiCl_2$(OMe) [18]. Complex **1** reacts with K[O^{t}Bu] in toluene at 20 °C to yield a mixture of **2** [8] and Tp^{Ms*}Ti(III)Cl_2(pz^{Ms}) [19] rather than the expected $Tp^{Ms*}TiCl_2(O^tBu)$ [20]. However, **1** does react with K[O-2,4,6-^{t}Bu$_3$-Ph] to afford **3** in 73% isolated yield. An X-ray diffraction analysis of **3** showed that the bulky –OAr group is *cis* to the 5-Ms-pyrazolyl ring of the Tp^{Ms*} ligand and that the metal center is very crowded [21]. The NMR spectrum of **3** shows that rotation of the mesityl and aryloxide rings is restricted.

3.2. Olefin polymerization studies

Precatalysts **1**–**6** were activated with DMAO in toluene and their ethylene homopolymerization and ethylene/α-olefin copolymerization behavior was investigated.

3.2.1. Ethylene homopolymerization

Ethylene homopolymerization results are summarized in Table 1. A low catalyst loading but high Al/catalyst ratio was used in these experiments to minimize mass transport and temperature control problems and broadening of the MWDs due to chain transfer to Al [6a,9]. Several measures of productivity based on ethylene consumption are listed in Table 1. The productivity based on cumulative ethylene consumption after 5 min (P_{5min} (kg polymer)/[(mmol M)(h)]) (M = metal) is a rough measure of activity. At this point, the effects of mass transport limitations and catalyst decomposition should be minor for most cases up to 100 °C. The productivity based on cumulative ethylene consumption at the end of the polymerization time (P_{end} (kg polymer)/[(mmol M)(h)]) reflects the activity and stability of the catalysts and mass transport effects. To

Table 1
Ethylene polymerization by **1**–**6**/DMAO[a]

Entry	Complex	T_p (°C)	Yield (g)	P_{5min}[b]	P_{end}[c]	k_p[d] (s^{-1} M^{-1})	k_d[e] (10^{-3} s^{-1})	P_{norm}[f]	M_v[g] (10^3)	T_m (°C)
1	**1**	60	0.168	9.6	12.2	112.0 ± 1.2	−0.05 ± 0.02	24.6	4186	135.1
2	**1**	80	0.229	17.9	18.0	218.8 ± 2.5	0.00 ± 0.02	41.8	1175	–
3	**1**	100	0.186	17.2	12.8	267.1 ± 3.0	0.72 ± 0.03	41.6	144	–
4	**1**	120	0.186	21.0	12.4	473.2 ± 2.7	1.68 ± 0.02	35.8	89	–
5	**1**	140	0.064	18.3	7.0	920.6 ± 14.0	6.22 ± 0.11	21.6	85	133.5
6	**2**	60	0.427	36.1	29.4	345.7 ± 1.9	0.35 ± 0.01	62.6	2108	135.4
7	**2**	80	0.527	68.0	38.2	979.6 ± 11.3	1.57 ± 0.04	96.5	625	–
8	**2**	100	0.407	44.2	30.4	720.1 ± 8.9	0.91 ± 0.03	91.1	188	–
9	**2**	120	0.162	34.4	14.8	1014.2 ± 11.8	3.63 ± 0.05	44.2	259	–
10	**2**	140	0.055	13.6	5.0	881.8 ± 15.9	8.48 ± 0.17	18.6	244	134.2
11	**3**	60	0.127	9.7	8.6	96.4 ± 0.4	0.26 ± 0.01	18.6	6825	134.2
12	**3**	80	0.103	4.9	5.1	65.7 ± 0.7	0.22 ± 0.02	18.8	3918	134.4
13	**3**	100	0.036	1.4	0.7	28.7 ± 0.7	2.64 ± 0.09	8.1	2163	134.2
14	**3**	120	0.042	2.5	2.3	62.9 ± 1.0	2.24 ± 0.05	11.4	392	130.6
15	**3**	140	0.033	3.3	1.5	137.8 ± 4.6	2.98 ± 0.14	11.2	–	131.1
16	**4**	60	0.645	82.6	50.3	919.3 ± 11.9	1.31 ± 0.04	94.5	2485	134.2
17[h]	**4**	60	0.361	255.8	159.9	728.2 ± 1.5	1.23 ± 0.01	264.1	3125	–
18	**4**	80	0.380	56.7	28.5	908.1 ± 17.1	2.22 ± 0.07	69.6	1381	–
19	**4**	100	0.267	45.2	20.8	971.7 ± 19.2	2.74 ± 0.08	59.7	1006	–
20	**4**	120	0.117	26.0	9.9	705.5 ± 9.4	3.55 ± 0.06	32.0	512	–
21	**4**	140	0.028	10.0	3.0	575.9 ± 11.8	7.37 ± 0.17	9.3	731	134.4
22[i]	**5**	60	0.377	47.9	37.2	613.0 ± 6.4	1.84 ± 0.05	92.0	3874	133.6
23[h]	**5**	60	0.472	273.7	207.4	728.9 ± 2.2	0.69 ± 0.01	346.0	5704	–
24[i]	**5**	80	0.306	49.5	31.2	965.9 ± 6.1	3.30 ± 0.03	93.3	2860	–
25[i]	**5**	100	0.256	43.7	23.2	1509.8 ± 25.7	6.51 ± 0.14	95.3	1129	–
26[i]	**5**	120	0.108	29.8	15.4	1611.9 ± 17.7	9.02 ± 0.11	49.1	998	–
27[i]	**5**	140	0.038	11.3	4.8	958.8 ± 8.5	11.94 ± 0.12	21.3	531	133.6
28	**6**	60	0.455	49.0	37.4	526.8 ± 4.6	0.71 ± 0.02	66.6	4529	135.1
29	**6**	80	0.250	43.1	17.5	829.5 ± 15.2	3.51 ± 0.08	45.8	1479	–
30	**6**	100	0.129	34.8	10.3	1783.5 ± 38.7	10.25 ± 0.24	28.8	1802	–
31	**6**	120	0.067	16.1	5.4	678.4 ± 14.2	6.01 ± 0.14	18.2	392	–
32	**6**	140	0.021	6.3	1.8	455.0 ± 13.4	9.37 ± 0.29	7.0	615	134.6

[a] Polymerization conditions: Argonaut parallel pressure reactor, 5 mL toluene, $P_{C_2H_4}$ = 9.68 atm, 0.02 μmol complex, 0.15 mmol DMAO, polymerization time: 20 min for all entries except 22 and 24–27, for which polymerization time = 12 min. Complex/toluene solution was injected into DMAO/toluene solution in Argonaut parallel pressure reactor at 9.68 atm ethylene pressure to start reaction.

[b] P_{5min} = kg polymer/[(mmol complex)(h)] = productivity based on cumulative ethylene uptake after 5 min.

[c] P_{end} = kg polymer/[(mmol complex)(h)] = productivity based on cumulative ethylene uptake at the end of the reaction (12 min for entries 22, 24–27 and 20 min for the others).

[d] k_p = propagation rate constant determined from kinetic profiles in Fig. 4 as described in the text.

[e] k_d = deactivation rate constant determined from kinetic profiles in Fig. 4 as described in the text.

[f] P_{norm} = kg polymer/[(mmol M)([ethylene])(h)] = productivity based on polymer yield and ethylene concentration.

[g] M_v = viscosity average molecular weight determined by intrinsic viscosity measurement.

[h] Catalyst loading: 0.004 μmol Zr, 0.15 mmol DMAO; polymerization time: 20 min.

[i] Reaction terminated at 12 min due to excessive stirring load.

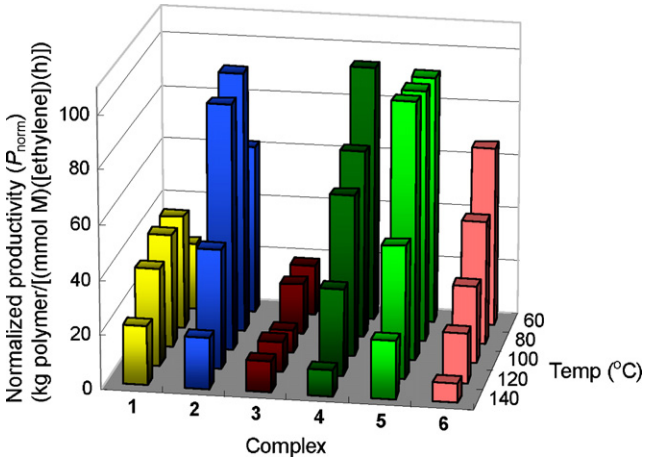

Fig. 2. Normalized productivities (P_{norm}) in ethylene polymerization at 60–140 °C by **1**–**6**/DMAO.

better understand temperature effects, values for the normalized productivity based on polymer yield after the end of the polymerization time and ethylene concentration (P_{norm} (kg polymer)/[(mmol M)([ethylene])(h)]) were determined [22]. P_{norm} values are listed in Table 1 and summarized in Fig. 2. M_v values for the PE products are shown in Fig. 3.

Kinetic profiles for ethylene polymerizations are shown in Fig. 4. These data were analyzed using a simple kinetic model that assumes that (i) the catalyst is rapidly and completely activated and (ii) propagation and deactivation are both first order in catalyst. Assumption (i) is reasonable since the instantaneous ethylene uptake rate is high initially and does not increase as the reaction proceeds. Assumption (ii) is reasonable since reduction in catalyst concentration by a factor of 5 resulted in only small changes in k_p and k_d values (*vide infra*; see Table 1 entries 16 versus 17 and 22 versus 23).

Under these conditions, the rate law for propagation is given by Eq. (1), where $C2_t$ is the cumulative ethylene consumption in time t, cat_t is the concentration of active catalyst at time t, and

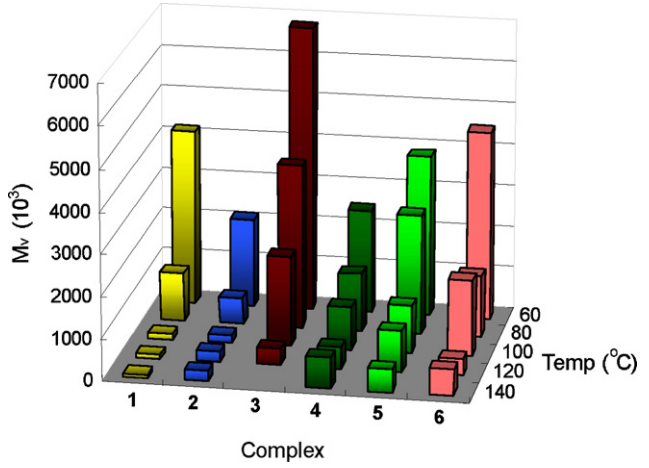

Fig. 3. Viscosity average molecular weight (M_v) of polyethylene produced by **1**–**6**/DMAO.

$k_{p,obs}$ is the first order rate constant for propagation.

$$\frac{dC2_t}{dt} = k_{p,obs}\, cat_t \quad (1)$$

The rate law for catalyst deactivation is given by Eqs. (2) and (3), where k_d is the rate constant for deactivation and cat_0 is the initial concentration of the catalyst.

$$\frac{-dcat_t}{dt} = k_d\, cat_t \quad (2)$$

$$cat_t = cat_0\, \exp(-k_d t) \quad (3)$$

Substitution of Eq. (3) into Eq. (1) gives Eq. (4), to which the observed ethylene uptakes were fit to determine values for $k_{p,obs}$ and k_d [23].

$$C2_t = cat_0\, k_{p,obs}[1 - \exp(-k_d t)]/k_d \quad (4)$$

Assuming that propagation is first order in ethylene, the second order rate constant for propagation is given by Eq. (5).

$$k_p = \frac{k_{p,obs}}{[ethylene]} \quad (5)$$

Values for k_p and k_d are listed in Table 1 and shown in Figs. 5 and 6.

*3.2.1.1. Influence of metal (Ti, Zr, Hf): comparison of **1**, **4** and **6**.* Complexes **1** (Ti), **4** (Zr), **6** (Hf) contain the same Tp′ ligand and offer an opportunity to probe the effect of metal on polymerization performance. At 60 °C, the productivities vary in the order **4** > **6** > **1** (Table 1, entries 1, 16, 28; Fig. 2). This trend largely reflects the variation in k_p (Fig. 5) because catalyst deactivation is slow at this temperature (Fig. 6). However, productivities fall off significantly with increasing temperature for **4** and **6**, and at 140 °C the productivity order is **1** > **4** > **6** (Table 1, entries 5, 21, 32; Fig. 2). In all three cases, k_d increases with increasing temperature, but for **4** and **6**, k_p reaches a maximum value at 100 °C whereas for **1**, k_p increases monotonically with temperature.

Catalyst **1**, **4**, and **6** all produce high molecular weight, linear PE at 60 °C ($M_v > 2.5 \times 10^6$). However, M_v falls off rapidly with increasing temperature, especially for **1** (Table 1 and Fig. 3).

*3.2.1.2. Influence of Ti (IV) and Ti(III) oxidation states: comparison of **1** and **2**.* Complexes **1** (Ti(IV)) and **2** (Ti(III)) contain the same ligand set but differ in the oxidation state at Ti. The productivity of **2** is higher than for **1** up to 120 °C, above which point the productivities of **1** and **2** are similar (Table 1 and Fig. 2). For both catalysts, k_d increases with increasing temperature, but for **2**, k_p plateaus (at a high value) above 80 °C whereas for **1**, k_p increases monotonically with temperature as noted above.

The M_vs produced by **2** are lower than those by **1** up to 80 °C (Fig. 3), which is consistent with previous results [8]. However above this temperature the order is reversed. **2** also produced highly linear PE.

*3.2.1.3. Influence of Tp' ligand structure: comparison of **4** and **5**.* Complexes **4** (Tp^{Ms}) and **5** (Tp^{Ms*}) differ in the location of the Ms substituents on the Tp′ ligand, with **5** being more crowded

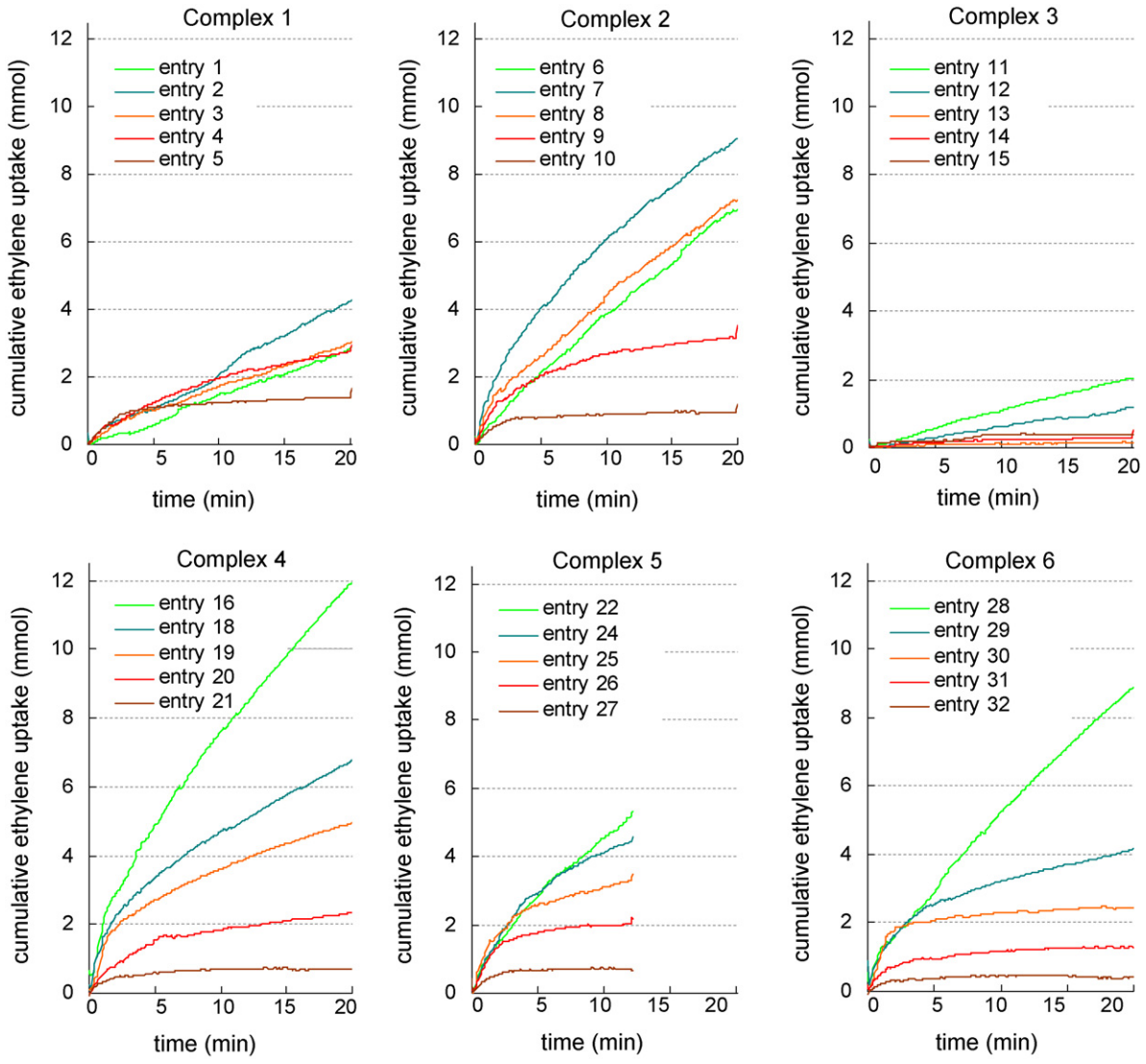

Fig. 4. Kinetic profiles of ethylene polymerization by **1**-**6**/DMAO. Entry designations refer to Table 1.

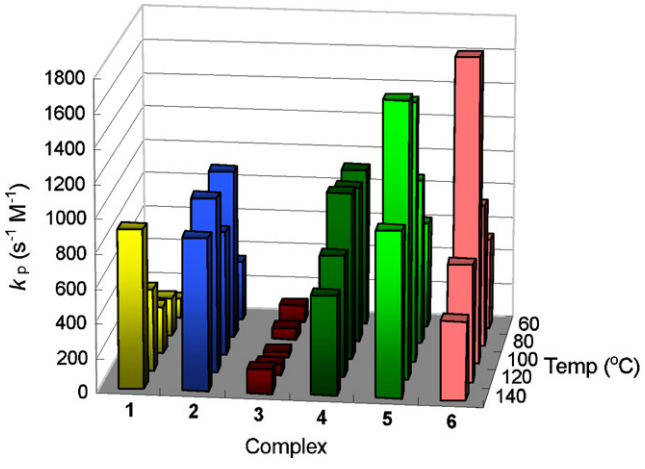

Fig. 5. Rate constants for propagation (k_p) of ethylene polymerization at 60–140 °C by **1**–**6**/DMAO.

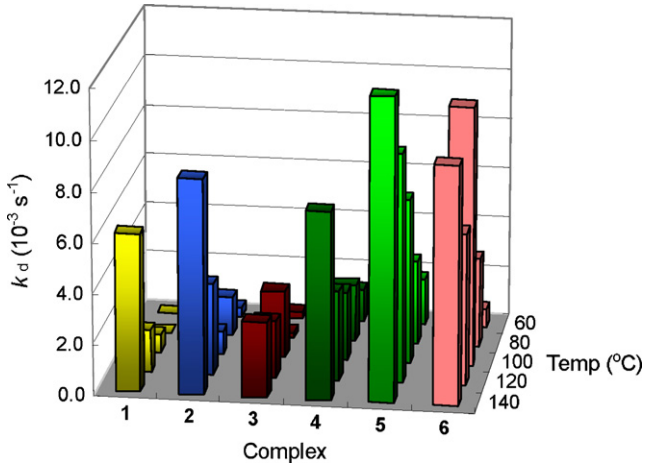

Fig. 6. Rate constants for catalyst deactivation (k_d) of ethylene polymerization at 60–140 °C by **1**–**6**/DMAO.

Table 2
Ethylene/1-hexene copolymerization by **1–6**/DMAO[a]

Entry	Complex	Complex load (μmol)	DMAO load (mmol)	T_p (°C)	Yield (g)	P_{yield}[b]	M_w[c] (10^3)	M_w/M_n	Hexene[d] (mol%)	$r_E \times r_H$
1	**1**	0.02	0.15	80	0.015	4.56	–	–		
2	**1**	0.02	1.50	80	0.011	3.26	21	1.6	10.0	1.49
3	**1**	0.02	0.15	60	0.025	7.62	1690	1.6	2.9	0.05
4	**1**	0.02	1.50	60	0.051	15.26	–	–		
5	**2**	0.02	0.15	80	0.141	42.27	241	2.3		
6	**2**	0.02	1.50	80	0.140	41.87	20	2.1	16.0	0.87
7	**2**	0.02	0.15	60	0.300	89.97	446	2.9	11.6	0.46
8	**2**	0.02	1.50	60	0.289	86.81	36	1.9		
9	**3**	0.02	0.15	80	Trace	<1	870	2.4		
10	**3**	0.02	1.50	80	0.032	9.47	–	–	5.2	0.40
11	**3**	0.2	0.15	80	0.052	1.56	508	2.4		
12	**3**	0.2	1.50	80	0.099	2.96	15	1.9	12.8	0.92
13	**4**	0.02	0.15	80	0.025	7.41	1070	28.5		
14	**4**	0.02	1.50	80	0.024	7.28	1280	23.0	27.9	0.33
15	**5**	0.02	0.15	80	0.161	48.15	2360	2.7		
16	**5**	0.02	1.50	80	0.156	46.67	1310	2.2	40.9	0.10
17	**6**	0.02	0.15	80	0.033	9.87	304	3.3		
18	**6**	0.02	1.50	80	0.042	12.71	25	1.8	10.3	0.94
19	Cp_2ZrCl_2	0.02	0.15	80	0.049	14.58	2	1.9		
20	Cp_2ZrCl_2	0.02	1.50	80	0.149	44.84	2	1.9	34.6	0.41

[a] Polymerization conditions: Argonaut parallel pressure reactor, 2 mL toluene, $P_{C_2H_4}$ = 0.967 atm, hexene = 3 mL, polymerization time 10 min. Precatalyst/toluene solution was injected into DMAO/toluene solution in Argonaut parallel pressure reactor at 0.967 atm ethylene pressure to start reaction.
[b] P_{yield} = kg polymer/[(mmol M)(h)] = productivity based on polymer yield.
[c] M_w = weight average molecular weight determined by GPC, reported using polystyrene calibration.
[d] Hexene incorporation determined by ^{13}C NMR using an JEOL EX400 instrument (100 MHz).

at the Zr center than **4**. Under the standard conditions used in this study, polymerizations with **5** were restricted to 12 min runs, due to a high stirring load resulting from a high yield of high molecular weight polymer. Therefore, the P_{5min} values provide the most useful measure of comparative productivity for this pair of catalysts. These data show that **4** is more productive than **5** at 60 °C but that the productivities of the two catalysts are very similar at 80 °C and above. At 80 °C and above, both k_p and k_d are higher for **5** than **4**. To obtain a comparison of these catalysts that is not complicated by possible mass transport effects, polymerizations were run at 60 °C with a very low catalyst loading (0.004 μmol Zr, 20 min run; Table 1, entries 17 and 23). Under these conditions, **5** exhibited somewhat higher productivity (P_{5min}, P_{end}, P_{norm}) than **4**, due to a lower k_d. Complex **5** gave a higher M_v than **4** under most conditions (Fig. 3), possibly due to steric inhibition of chain transfer to Al.

*3.2.1.4. Influence of aryloxide substituent: comparison of **1** and **3**.* Complex **3** is significantly more crowded than **1** due to the presence of the bulky aryloxide ligand [21]. The electronic properties of **1** and **3** may also differ, although little is known about this issue at present. Complex **3** is less active than **1** under all conditions studied, primarily due to low k_p values. However, **3** gave the highest M_v among all of the catalysts studied between 60 and 100 °C (Fig. 3) [24]. These results suggest that the aryloxide ligand is retained in the active form of **3** and the resulting extreme steric crowding inhibits propagation by hindering access of ethylene monomer to the Ti center, and inhibits chain transfer by hindering access of Al alkyl species to the Ti center.

3.2.2. Ethylene/1-hexene copolymerization

The ethylene/1-hexene copolymerization behavior of **1–6** was studied at 80 °C (and in some cases 60 °C) at two different DMAO levels (0.15 mmol, same as for ethylene homopolymerizations, and 1.5 mmol). The productivities based on polymer yield after the end of the polymerization time (P_{yield} (kg polymer)/[(mmol M)(h)]), polymer molecular weights, and hexene content data, are summarized in Table 2 and Figs. 7–9.

*3.2.2.1. Influence of metal (Ti, Zr, Hf): comparison of **1**, **4** and **6**.* The ethylene/1-hexene copolymerization productivity at 80 °C varies in the order **1** < **4** < **6**; as for ethylene homopolymerization, the Ti catalyst is the least productive. Catalysts **1** and **6** both produce low molecular weight copolymer (M_w ca. 23 × 10^3, MWD

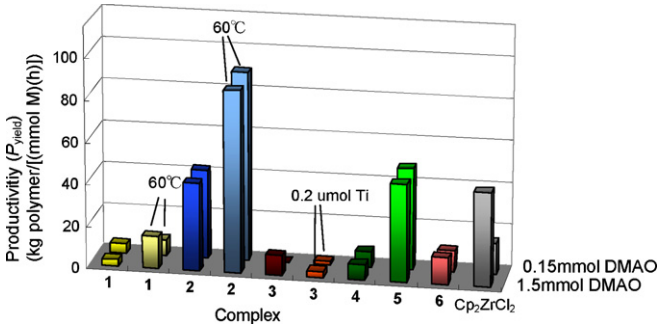

Fig. 7. Productivity (P_{yield}) of ethylene/1-hexene copolymerization by **1–6**/DMAO. Polymerization conditions: 0.02 μmol complex except where indicated, 0.15 mmol DMAO, 5 mL toluene, 0.967 atm ethylene, 3 mL hexene, 10 min, 80 °C except where indicated.

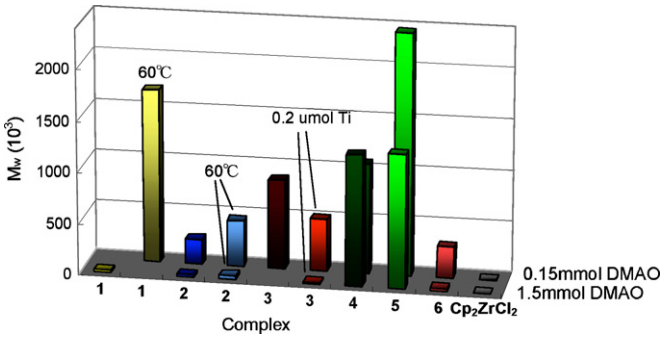

Fig. 8. Weight average molecular weight (M_w) of ethylene/1-hexene copolymer produced by **1**–**6**/DMAO. Polymerization conditions are the same as for Fig. 7.

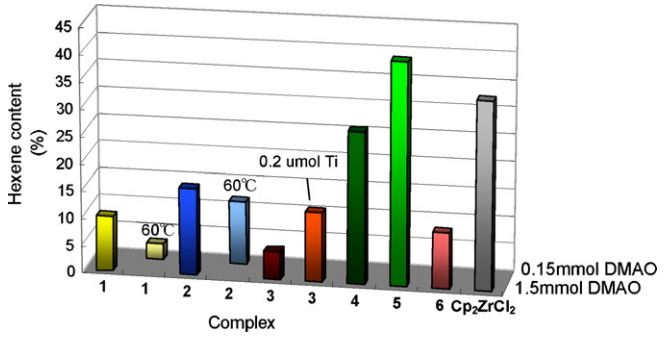

Fig. 9. Hexene content of ethylene/1-hexene copolymer produced by **1**–**6**/DMAO. Polymerization conditions are the same as for Fig. 7.

ca. 2) with ca. 10% hexene incorporation at the higher DMAO loading of 1.5 mmol. At the lower DMAO level, the M_ws are higher, consistent with chain transfer to Al being an important chain transfer mechanism (e.g. Table 2, entry 17 versus 18).

The behavior of **4** is quite different however. At 80 °C and DMAO = 1.5 mmol, **4** produces much higher molecular weight copolymer ($M_w = 1.3 \times 10^6$) with much higher hexene incorporation (28 %) compared to **1** and **6**. However, GPC analysis [23] shows that the copolymer from **4** has a broad bimodal MWD. CFC analysis [23] shows that this material has a broad composition distribution and contains a high molecular weight hexene-rich fraction and a low molecular weight fraction with a lower hexene content. These observations imply that multiple active species are generated from **4**. Interestingly, reduction of the DMAO level by a factor of 10 does not influence the M_w or MWD for **4** (Table 2, entry 13 versus 14), in direct contrast to the significant reduction in M_w for **1** and **6** noted above (Table 2, entry 17 versus 18).

*3.2.2.2. Influence of Ti (IV) and Ti(III) oxidation states: comparison of **1** and **2**.* Ti(III) complex **2** exhibits much higher productivity (Table 2, entries 5–8) and higher hexene incorporation in ethylene/hexene copolymerization compared to Ti(IV) complex **1** (Table 2, entries 1–4) under the studied conditions. Previous work showed that **1** exhibits similar productivity to **2** at low MAO levels but is more susceptible to deactivation by alkylaluminum [8]. The low productivity for **1** observed here (at relatively high DMAO levels) is consistent with these results. The M_ws of the ethylene/1-hexene copolymers produced by **2** are higher at lower DMAO levels, again consistent with chain transfer to Al being a dominant chain transfer mechanism.

*3.2.2.3. Influence of Tp' ligand structure: comparison of **4** and **5**.* The copolymerization productivity of **5** is ca. seven times higher than that of **4** (Table 2, entries 15 and 16 versus 13 and 14), in contrast to the similar productivities observed for these catalysts in ethylene homopolymerization. Complex **5** also exhibits higher hexene incorporation (41%) than **4** (entry 14 versus 16), despite the greater steric crowding in **5**. In fact, the hexene content for **5** was the highest among the catalysts examined. Both **4** and **5** gave copolymers with high M_w. However, the MWDs for **5** are narrow in contrast to the broad MWDs noted above for **4**. Additionally, CFC analysis of the copolymer from **5** (entry 16) showed that the entire copolymer elutes at 0 °C, which establishes that a low hexene fraction is not present, in contrast to the results for **4** noted above. The M_ws from **4** and **5** are high at both low and high DMAO loadings.

NMR analysis of the ethylene/1-hexene copolymer produced by **5** [23] revealed a moderately alternating sequence distribution ($r_E \times r_H = 0.10$) [25]. Regioerrors were not observed.

*3.2.2.4. Influence of aryloxide substituent: comparison of **1** and **3**.* The copolymerization behavior of **3** is similar to that of **1** despite the presence of the aryloxide group. Both catalysts exhibit modest productivity, modest hexene incorporation levels and significant reduction in M_w at the higher DMAO level.

Table 3
Ethylene/propylene copolymerization by **5**/DMAO[a]

Entry	Complex	DMAO (mmol)	$P_{C_3H_6}$ (atm)[b]	Total pressure (atm)[c]	Yield (g)	P_{yield}[d]	M_w[e] (10^3)	M_w/M_n	Propylene (mol%)[f]	$r_E \times r_H$
1	**5**	1.50	3.87	9.68	0.167	50.16	1390	6.6	34.7	0.30
2	**5**	0.15	3.87	9.68	0.203	60.81	3100	10.6	35.0	0.35
3	**5**	0.15	3.87	8.71	0.060	17.43	358	3.6	52.0	0.28

[a] Polymerization conditions: Argonaut parallel pressure reactor, 5 mL toluene, 0.02 μmol Zr, $T_p = 80$ °C, polymerization time 10 min. Complex/toluene solution was injected into DMAO/toluene solution in Argonaut parallel pressure reactor at polymerization pressure to start reaction.
[b] Initial propylene pressure at 25 °C.
[c] Total pressure at 80 °C.
[d] P_{yield} = kg polymer/[(mmol M)(h)] = productivity based on polymer yield.
[e] M_w = weight average molecular weight determined by GPC versus polystyrene calibration.
[f] Propylene incorporation determined by ^{13}C NMR.

3.2.2.5. Comparative behavior of Cp_2ZrCl_2. The copolymerization performance of Cp_2ZrCl_2 was investigated under the standard conditions used here to provide a benchmark for assessment of the performance of **5**. The data are summarized in Table 2 (runs 19, 20) and Figs. 7–9. Although Cp_2ZrCl_2 exhibits comparable hexene incorporation, it exhibits lower activity (especially at the low DMAO loading), and much lower M_w compared to **2** and **5**.

3.2.3. Ethylene/propylene copolymerization by 5

The ethylene/propylene copolymerization behavior of **5**/DMAO was investigated to probe if the tendency for an alternating sequence distribution in ethylene/hexene copolymerization would also be observed for the smaller comonomer propylene. The results are shown in Table 3 [26]. Complex **5** produces copolymers with up to 52 mol% propylene, and the sequence distribution is somewhat less alternating than observed for ethylene/hexene copolymers [23,27]. Complex **5** produces less-alternating ethylene/propylene copolymer than C_1-symmetric metallocenes, but offers the potential advantage of being able to produce very high molecular weight copolymer [28].

4. Summary

These studies provide a comparison of the olefin polymerization performance of sterically crowded group 4 metal Tp'MX_3/DMAO catalysts. Diverse behavior is observed for Tp'MX_3 complexes with different metals, oxidation states, Tp' ligands and X substituents.

The order of productivity in ethylene polymerization at $T_p = 60\,^\circ C$ is: **5** > **4** > **6**, **2** > **1** > **3**. These catalysts all produce linear PE with $M_v > 10^6$ at 60 °C, and **3**–**6** produce PE with $M_v > 10^6$ even up to 100 °C. For the $Tp^{Ms*}MCl_3$ catalysts **1** (Ti), **4** (Zr) and **6** (Hf), the productivity order is Zr > Hf > Ti at 60 °C but Ti > Zr > Hf at 140 °C. The order changes because k_p increases monotonically with temperature for **1** but peaks at 100 °C for **4** and **6**. The activity of the Tp^{Ms*}Ti(III) catalyst **2** is generally higher than that of Tp^{Ms*}Ti(IV) catalyst **1**. $Tp^{Ms}ZrCl_3$ (**5**) is more productive and produces higher molecular weight PE than the less-crowded isomer Tp^{Ms}*$ZrCl_3$ (**4**). Incorporation of a bulky aryloxide ligand in **3** does not increase productivity in ethylene polymerization.

The order of productivity in ethylene/1-hexene copolymerization at $T_p = 80\,^\circ C$ is: **5**, **2** > **6**, **3**, **4** > **1**. Hexene incorporation increases in the order **5**, **4** > **2** > **3**, **1**, **6**. The Zr catalysts **4** and **5** produce high M_w copolymer at both low and high DMAO levels; in contrast, for the other catalysts M_w decreases significantly at high DMAO levels, most likely due to chain transfer to Al. The copolymer produced by **4** has a broad bimodal MWD and broad composition distribution indicative of the presence of multiple active species. In contrast, **5** displays single-site behavior in ethylene/hexene copolymerization. At 80 °C, **5** produces moderately alternating ethylene/1-hexene copolymer (41 mol% hexene) with ultra-high molecular weight ($M_w = 1.3 \times 10^6$), narrow MWD (2.2) and narrow composition distribution with high efficiency.

Development of a mechanistic understanding of these observations will require extensive work to identify the active species in these catalysts.

Acknowledgements

This work was supported by the U.S. Department of Energy (DE-FG-02-00ER15036) and Mitsui Chemicals, Inc. (Japan). We thank Dr. Y. Suzuki for fruitful discussions and suggestions on kinetic analysis. We also thank Mitsui Chemical Analysis & Consulting Service, Inc. (Japan), for FD-MS, intrinsic viscosity, GPC, and NMR measurements.

Appendix A. Supplementary data

Supplementary data associated with this article can be found, in the online version, at doi:10.1016/j.molcata.2007.11.023.

References

[1] W. Kaminsky, J. Polym. Sci. Part A: Polym. Chem. 42 (2004) 3911, references therein.
[2] V.C. Gibson, S.K. Spitzmesser, Chem. Rev. 103 (2003) 283, references therein.
[3] (a) S. Trofimenko, Scorpionates: The Coordination Chemistry of Polypyrazolylborate Ligands, Imperial College Press, London, 1999;
(b) S. Trofimenko, Chem. Rev. 93 (1993) 943;
(c) D.M. Tellers, S.J. Skoog, R.G. Bergman, T.B. Gunnoe, W.D. Harman, Organometallics 19 (2000) 2428.
[4] (a) H. Nakazawa, S. Ikai, K. Imaoka, Y. Kai, T. Yano, J. Mol. Catal. A: Chem. 132 (1998) 33;
(b) T. Obara, S. Ueki, JP patent 1989095110 (1989), to Tonen Corporation.;
(c) K.J. Jens, M. Tilset, A. Heuman, WO patent 97/17379 (1997), to Borealis.;
(d) P.T. Matsunaga, S. Rinaldo, WO patent 99/29739 (1999), to Exxon.;
(e) H. Nakazawa, S. Ikai, K. Imaoka, E. Ogawa, JP1996127610 (1996), to Ube Ind.
[5] For Cp'Tp'ZrX_2 catalysts (Cp' = C_5H_5 or C_5Me_5; Tp' = Tp, Tp*, ^{Bu}Tp (^{Bu}Tp = BuB(pyrazolyl)$_3$)), see:
(a) S.-J. Wang, Y.-C. Chen, S.-H. Chain, J.-C. Tsai, Y.-H.E. Sheu, US Patent 5,519,099 (1999), to Industrial Technology Research Institute (Taiwan).;
(b) T. Yorisue, S. Kanejima, JP patent 1996027210 (1996), to Asahi Kasei.;
(c) F. Matsushita, F. Yamaguchi, T. Izuhara, JP patent 1996059746 (1996), to Asahi Kasei.;
(d) T. Aoki, T. Kaneshima, Eur. Patent 0,617,052 (1994), to Asahi Kasei.
[6] (a) S. Murtuza, O.L. Casagrande Jr., R.F. Jordan, Organometallics 21 (2002) 1882;
(b) K. Michiue, I.M. Steele, O.L. Casagrande Jr., R.F. Jordan, Acta Cryst. E62 (2006) m2297.
[7] L.G. Furlan, M.P. Gil, O.L. Casagrande Jr., Macromol. Rapid Commun. 21 (2000) 1054.
[8] K. Michiue, R.F. Jordan, Macromolecules 36 (2003) 9707.
[9] K. Michiue, R.F. Jordan, Organometallics 23 (2004) 460.
[10] M.P. Gil, O.L. Casagrande Jr., J. Organomet. Chem. 689 (2004) 286.
[11] (a) A. Karam, M. Jimeno, J. Lezama, E. Catari, A. Figueroa, B.R. de Gascue, J. Mol. Catal. A: Chem. 176 (2001) 65;
(b) S. Ikai, Y. Kai, M. Murakami, H. Nakazawa, JP patent 1999228614 (1999), to Ube Ind.;
(c) H. Nakazawa, S. Ikai, K. Imaoka, Y. Kai, N. Mitani, JP patent 1996253524 (1996), to Ube Ind.;
(d) T.H. Newman, Eur. Patent 0,482,934 (1992), to Dow Chemical Company.
[12] A. Karam, E. Casas, E. Catarí, S. Pekerar, A. Albornoz, B. Méndez, J. Mol. Catal. A: Chem. 238 (2005) 233.

[13] H. Lee, R.F. Jordan, J. Am. Chem. Soc. 127 (2005) 9384.
[14] M.J. Yanjarappa, S. Sivaram, Prog. Polym. Sci. 27 (2002) 1347.
[15] M.P. Gil, J.H.Z. dos Santos, O.L. Casagrande Jr., Macromol. Rapid Commun. 202 (2001) 319.
[16] K. Michiue, R.F. Jordan, JP patent 2005239910 (2005), to Mitsui Chemicals, Inc.
[17] R. Chiang, J. Polym. Sci. 36 (1959) 91.
[18] J. Ipaktschi, W. Sulzbach, J. Organomet. Chem. 426 (1992) 59.
[19] K. Michiue, I.M. Steele, R.F. Jordan, Acta Cryst. E62 (2006) m2357.
[20] For a similar reaction of Cp_2TiCl_2 see: A.W. Duff, R.A. Kamarudin, M.F. Lappert, R.J. Norton, J. Chem. Soc. Dalton Trans. 3 (1986) 489.
[21] K. Michiue, I.M. Steele, R.F. Jordan, Acta Cryst. E62 (2006) m2489.
[22] (a) Ethylene solubilities were calculated using the RK-SOAVE method as implemented in Aspen Plus®. For more details see: R.C. Reid, J.M. Prausnitz, B.E. Poling, The Properties of Gases and Liquids, fourth ed., MacGraw Hill, New York.;
(b) Calculated values are as follows: [Ethylene] (M) at 9.68 atm ethylene in toluene was estimated using Aspen Plus® as 1.024 (60 °C), 0.820 (80 °C), 0.670 (100 °C), 0.551 (120 °C), 0.446 (140 °C), respectively.;
(c) The calculated ethylene solubility agrees well with experimental data at 100 °C, but is slightly higher than the experimental value at 60 °C and slightly lower than the experimental values at 140 °C. See: L.-S. Lee, H.-J. Ou, H.-L. Hsu, Fluid Phase Equilibr. 231 (2005) 221.
[23] See supporting information for details.
[24] While the T_ms of PEs produced by **1**, **2**, and **4–6** were in the range of 133–135 °C characteristic of linear PEs (Table 1), the PEs produced by **3** had slightly reduced T_ms (run 14: 130.6 °C; run 15: 131.1 °C), similar to previously reported results for $TpTi(OMe)_{3-n}Cl_n$ ($n = 1,2$; ref. [11a]). This result suggests that a small amount of branching is present. However, branching was not detected by NMR.
[25] Triad distribution for Table 2, entry 16: [EHE] = 0.303, [EHH] = 0.106, [HHH] = 0.000, [HEH] = 0.254, [HEE] = 0.205, [EEE] = 0.133.
[26] Because a fixed limited quantity of propylene was used while ethylene was present at constant pressure on demand, broad MWDs and composition distributions are produced due to the change ethylene/propylene feed ratio during the reaction.
[27] Triad distribution for Table 3, entry 3: [EPE] = 0.226, [EPP] = 0.133, [PPP] = 0.122, [PEP] = 0.228, [PEE] = 0.148, [EEE] = 0.142.
[28] (a) B. Heuer, W. Kaminsky, Macromolecules 38 (2005) 3054;
(b) W. Fan, R.M. Waymouth, Macromolecules 36 (2003) 3010;
(c) T.N. Choo, R.M. Waymouth, J. Am. Chem. Soc. 124 (2002) 4188;
(d) W. Fan, R.M. Waymouth, Macromolecules 34 (2001) 8619;
(e) T. Uozumi, G.L. Tian, C.H. Ahn, J.Z. Jin, S. Tsubaki, T. Sano, K. Soga, J. Polym. Sci., Part A: Polym. Chem. 38 (2000) 1844;
(f) M.K. Leclerc, R.M. Waymouth, Angew. Chem. Int. Ed. 37 (1998) 922;
(g) J. Jin, T. Uozumi, T. Sano, T. Teranishi, K. Soga, T. Shiono, Macromol. Rapid Commun. 19 (1998) 337;
(h) M. Arnadt, W. Kaminsky, A.-M. Schauwienold, U. Weingarten, Macromol. Chem. Phys. 199 (1998) 1135;
(i) T. Uozumi, K. Miyazawa, T. Sano, K. Soga, Macromol. Rapid Commun. 18 (1997) 883;
(j) M. Galimberti, L. Resconi, E. Albizzati, EP patent 632066 (1995), to Montell technology Company;
(k) Z. Yu, M. Marques, M.D. Rausch, J.C.W. Chien, J. Polym. Sci., Part A: Polym. Chem. 33 (1995) 2795.